AUTHOR QUERY FOR GTMB-2010-0276-VER9-OTA_1P

AU1: Please italicize all the gene symbols mentioned in the article.

Malueka et al. BMC Genetics 2012, 13:23
http://www.biomedcentral.com/1471-2156/13/23

BMC Genetics

RESEARCH ARTICLE Open Access

Categorization of 77 *dystrophin* exons into 5 groups by a decision tree using indexes of splicing regulatory factors as decision markers

Rusdy Ghazali Malueka[1], Yutaka Takaoka[2], Mariko Yagi[1], Hiroyuki Awano[1], Tomoko Lee[1], Ery Kus Dwianingsih[1], Atsushi Nishida[1,3], Yasuhiro Takeshima[1] and Masafumi Matsuo[1,4*]

Abstract

Background: Duchenne muscular dystrophy, a fatal muscle-wasting disease, is characterized by dystrophin deficiency caused by mutations in the *dystrophin* gene. Skipping of a target *dystrophin* exon during splicing with antisense oligonucleotides is attracting much attention as the most plausible way to express dystrophin in DMD. Antisense oligonucleotides have been designed against splicing regulatory sequences such as splicing enhancer sequences of target exons. Recently, we reported that a chemical kinase inhibitor specifically enhances the skipping of mutated *dystrophin* exon 31, indicating the existence of exon-specific splicing regulatory systems. However, the basis for such individual regulatory systems is largely unknown. Here, we categorized the *dystrophin* exons in terms of their splicing regulatory factors.

Results: Using a computer-based machine learning system, we first constructed a decision tree separating 77 authentic from 14 known cryptic exons using 25 indexes of splicing regulatory factors as decision markers. We evaluated the classification accuracy of a novel cryptic exon (exon 11a) identified in this study. However, the tree mislabeled exon 11a as a true exon. Therefore, we re-constructed the decision tree to separate all 15 cryptic exons. The revised decision tree categorized the 77 authentic exons into five groups. Furthermore, all nine disease-associated novel exons were successfully categorized as exons, validating the decision tree. One group, consisting of 30 exons, was characterized by a high density of exonic splicing enhancer sequences. This suggests that AOs targeting splicing enhancer sequences would efficiently induce skipping of exons belonging to this group.

Conclusions: The decision tree categorized the 77 authentic exons into five groups. Our classification may help to establish the strategy for exon skipping therapy for Duchenne muscular dystrophy.

Keywords: Splicing, *Dystrophin*, Exon, Splicing enhancer, Decision tree

Background

Duchenne muscular dystrophy (DMD), a fatal muscle-wasting disease, is the most common inherited muscle disease, affecting one in every 3500 male births. DMD is characterized by dystrophin deficiency caused by mutations in the *dystrophin* gene, the largest human gene that spans over 2500 kb on the X-chromosome. For the treatment of DMD, antisense oligonucleotides (AOs) against splicing regulatory sequences have been proposed to produce in-frame *dystrophin* mRNA from the out-of-frame mRNA by inducing exon skipping during splicing [1]. The newly generated in-frame *dystrophin* mRNA is expected to produce semi-functional, internally deleted dystrophin protein. Currently, induction of exon skipping with AOs is considered one of the most promising treatments for DMD [2,3].

The *dystrophin* gene encodes a 14-kb mRNA consisting of 79 exons and is characterized by its huge intron size; the largest, intron 44, is 248 kb long. In addition, eight alternative promoters that are activated in a tissue-specific manner have been identified. Each tissue-specific exon 1 under the control of a cryptic promoter is spliced correctly

* Correspondence: mmatsuo@reha.kobegakuin.ac.jp
[1]Department of Pediatrics, Graduate School of Medicine, Kobe University, Chuo, Kobe 6500017, Japan
Full list of author information is available at the end of the article

to one of the downstream authentic *dystrophin* exons, producing a tissue-specific dystrophin isoform [4,5]. Furthermore, alternative splicings of some exons lead to the production of additional isoforms of the tissue-specific transcripts [6-8]. Remarkably, 14 cryptic exons that resemble authentic exons in terms of length and splice site strength, but are very rarely if ever spliced, have been reported within the huge introns [9,10].

Splicing is the process that removes introns from pre-mRNA, and is performed in the spliceosome, a ribonucleoprotein assembly. The spliceosome is one of the most complex cellular machineries, comprising approximately 150 proteins and five small nuclear RNAs (snRNAs U1, U2, U4, U5, and U6) [11]. Three sites, the splice donor site (5'ss), the splice acceptor site (3'ss), and the branch point sequences are the core splice site signals that are present in every intron. Despite the high potential for errors, the splicing process appears to occur with high fidelity, implying the widespread involvement of additional transcript features. These exonic elements are conventionally classified as exonic splicing enhancers (ESEs) or silencers (ESSs) and they function to promote or inhibit inclusion of the exon in which they reside, respectively. These splicing regulatory elements function by recruiting *trans*-acting splicing factors that activate or suppress splice site recognition or spliceosome assembly by various mechanisms [12]. AOs that induce skipping of *dystrophin* exons have been mainly designed against ESEs of target exons to hamper recruitment of splicing factors [2,3].

Recently, we reported that a small chemical enhances skipping of mutated *dystrophin* exon 31 in a sequence-specific manner, not altering the splicing of other *dystrophin* exons [13]. It was strongly suggested that *dystrophin* exons have their own splicing regulatory systems. However, the characteristics of the splicing regulatory systems of individual *dystrophin* exons are not well understood.

Decision trees are classifiers that predict class labels for data items and can make very accurate predictions [14,15]. They have been used to establish an integrated method that is one of the best available ways to find genes in the human genome [15].

Here, we identified a novel cryptic exon in intron 11 of the *dystrophin* gene in a DMD patient, and constructed decision trees to discriminate authentic exons from cryptic exons. Finally, we categorized 77 authentic exons into five groups based on indexes of their splicing regulatory factors. From the decision tree, we suppose that one group of exons showing high density for ESE sequences are a good target for exon skipping therapy.

Results

To examine the splicing regulatory factors that characterize particular exons, we constructed decision trees classifying authentic from cryptic exons using indexes of splicing regulatory factors as decision markers. Cryptic exons within the *dystrophin* gene resemble authentic exons in terms of length and splice site strength, but are very rarely if ever spliced [10]. Therefore, analyzing the exon recognition parameters of these exons compared to the authentic *dystrophin* exons can give insight into which splicing regulatory elements actually play a critical role in the splicing of *dystrophin* exons. The goal of the decision tree was to determine the critical parameters that provided the most accurate categorization of authentic exons and cryptic exons. A preliminary decision tree was constructed to discriminate 77 authentic exons from 14 known cryptic exons. To classify these exons, we used 26 indexes that have been reported as important in proper splicing (see Methods). The decision tree system output a simple data structure (Figure 1). The decision tree revealed that the strength of the 3'ss calculated by maximum entropy (ME3'ss) was the first splitting variable, with a cut-off point of 1.39. At this node, four cryptic exons were classified into one group. At the next node, SF2/ASF-D was used as the splitting variable, with a cut-off point of less than 10.44, generating a group of 32 authentic exons. In this way, seven nodes were used to separate clearly the 77 authentic exons from the 14 cryptic exons. The authentic exons were categorized into four groups, comprising 43, 32, 1, and 1 exon, respectively; similarly, the cryptic exons were also categorized into four groups.

We evaluated the decision tree by analyzing a novel cryptic exon 11a that was identified in this study. Exon 11a was found inserted into *dystrophin* mRNA in one DMD case who had a two-nucleotide (CA) deletion at the 5th and 6th nucleotides of exon 12 (c.1336_1337del). RT-nested PCR amplification of a fragment spanning exons 10 to 14 from this individual revealed two products: one corresponding to the normal size and the other larger than expected (Figure 2). Sequencing of the two products revealed that the normal-size band had the predicted exon content with the two-nucleotide deletion, and the larger product contained a 157-bp unknown insertion between exons 11 and 12. The inserted 157-bp sequence was identical to part of the 29.7-kb-long intron 11. The corresponding intronic sequence was present 5244 nt downstream of the 3' end of exon 11 and 24,278 nt upstream of exon 12 (Figure 2c). The inserted sequence maintained the AG and GT dinucleotide consensus sequences for splicing acceptor and donor sites at either end. Although the sequences flanking the inserted sequence were examined in this individual, no nucleotide change was found. The inserted sequence was named exon 11a.

When we tested exon 11a on our decision tree, it was classified not as a cryptic exon but as a real exon. Therefore, we decided that this tree was not suitable to classify

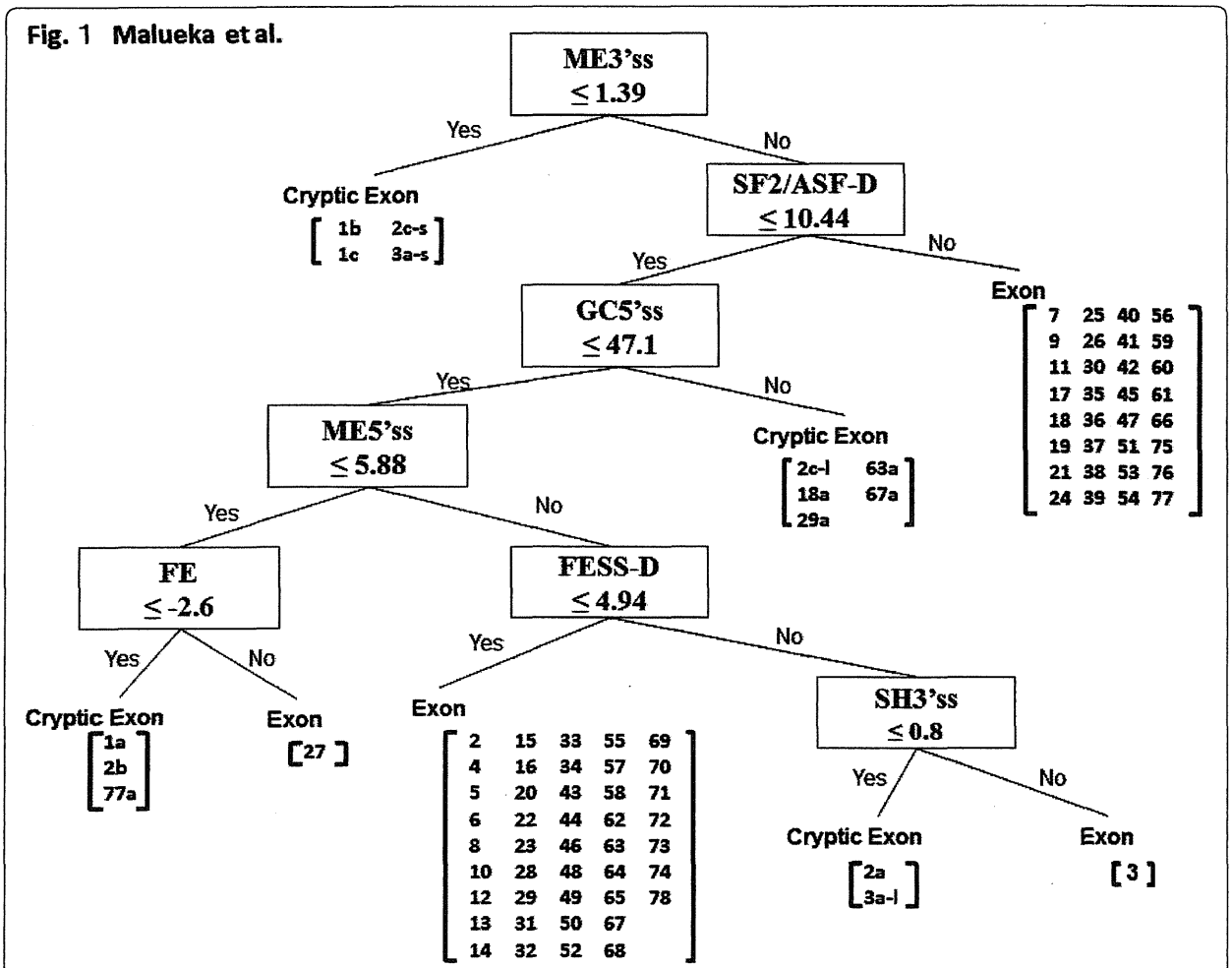

Figure 1 Preliminary decision tree to classify 77 authentic and 14 cryptic *dystrophin* exons. Exons are passed down the tree beginning at the top, where a "yes" result on any test means that it should be passed down to the left. The features tested in this tree are the maximum entropy at the 3' splice site (ss) (ME3'ss), the SF2/ASF density (SF2/ASF-D), the GC content at the 5'ss (GC5'ss), the maximum entropy at the 5'ss (ME5'ss), the free energy at the 5'ss U1 snRNP binding site (FE), the number of exonic splicing silencer (FESS), and the Shapiro score at the 3'ss (SH3'ss). The internal nodes of the tree represent index values that are tested for each exon as it is passed through the tree. Each successive node in the tree represents a decision that is based on those values, until a final classification is reached (the leaves). Authentic and cryptic exons were classified into four groups each.

exon 11a. We reconstructed the decision tree, including exon 11a as an additional cryptic exon using the same 26 indexes that were used to construct the first decision tree. The final tree, which had eight nodes, was able to separate all 15 cryptic exons from all 77 authentic exons with 100% accuracy (Figure 3). ME3'ss was the first splitting variable, with a cut-off point of 1.39. At this node, four cryptic exons were classified into one group (group a; Figure 3). SF2/ASF-D was the splitting variable at the second node, with a cut-off point of 10.53. A group of 32 exons (group A) was categorized on its "no" branch. Group A, therefore, was characterized by a high-density of ESEs recognized by SF2/ASF. At the third node, ME5'ss with a cut-off point of 5.58 was used to divide the data into two subnodes. On the "yes" branch, FE with a cut-off point of -2.6 split the group: one exon group consisting of five cryptic exons (group b) and one exon group containing only exon 27 (group B). On the other, "no" branch, FESS-D with a cut-off point of 4.45 divided the group into two subnodes. On the "yes" branch, GC5'ss with a cut-off point of 46.8 was used at the fifth node. One big exon group (group C), comprising 42 exons, formed the "yes" branch. On the other, "no" branch, SH3'ss with a cut-off point of 0.79 was used at the sixth node, generating a cryptic exon group (group c) and a group containing two authentic exons (exons 70

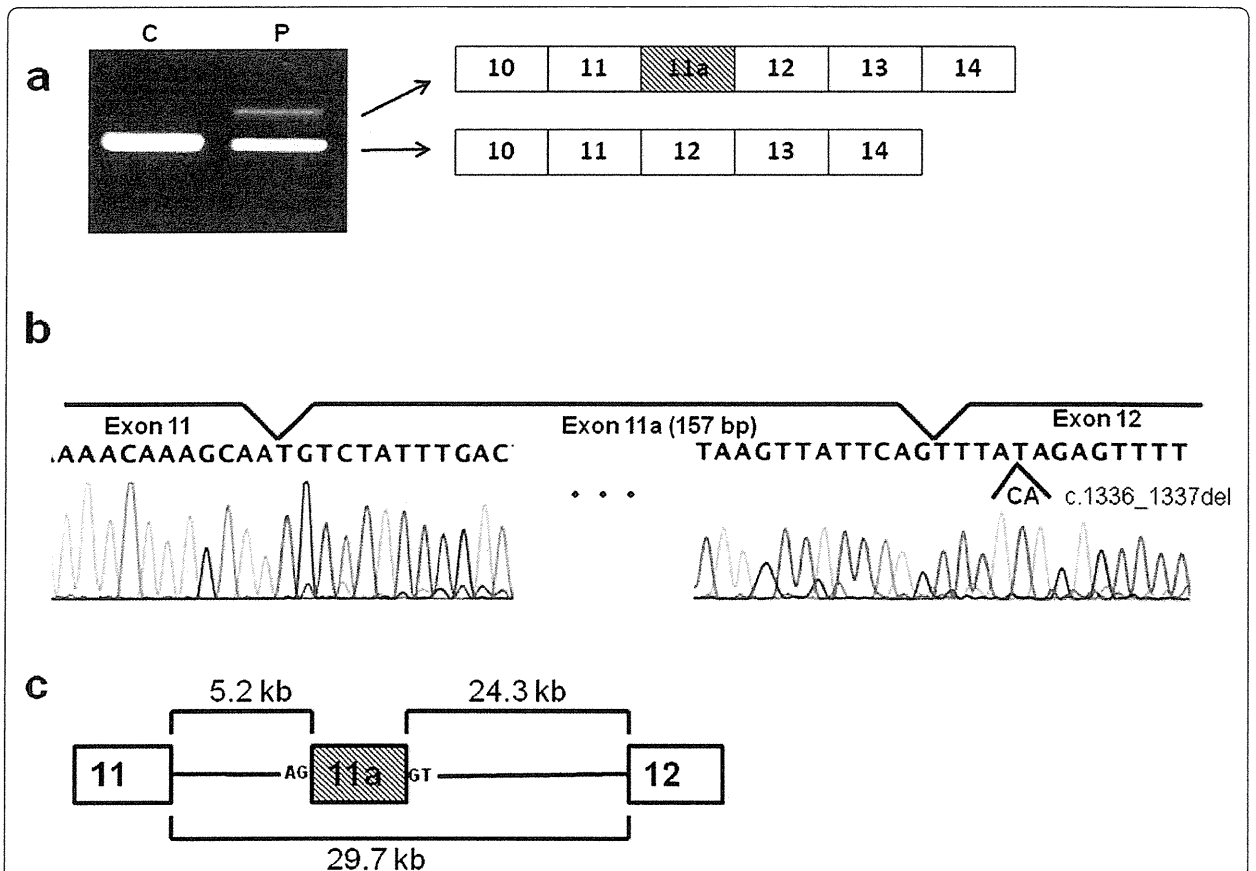

Figure 2 Cloning of cryptic exon 11a. a. RT-nested PCR products. A fragment spanning exons 10 to 14 was amplified by RT-nested PCR. Two amplified products were obtained from peripheral lymphocytes of a DMD patient (P) but not a control (C). A schematic representation of the exon structure of the amplified fragments is shown on the right. b. Sequences at the exon junctions. Subcloning and sequencing of the amplified products revealed that the larger product contained a 157-bp insertion (exon 11a) between exons 11 and 12. c. Schematic description of the location of exon 11a. The 5' and 3' ends of exon 11a (hatched box) are 5.2 kb downstream of exon 11, and 24.3 kb upstream of exon 12, respectively. Both the AG and GT splicing consensus dinucleotides are present adjacent to exon 11a.

and 78; group E). On the "no" branch at the fourth node, SIZE with a cut-off point of 144 was next used, categorizing the final data into one exon group consisting of exons 2 and 3 (group D) and one group containing four cryptic exons (group d).

We evaluated our re-constructed tree using nine disease-causing exons that have been identified in the *dystrophin* mRNAs of dystrophinopathy patients. These pathological exons are created by the effect of deep-intron single nucleotide mutations. These mutations confer the characteristics of an authentic exon on a portion of intronic sequence, and thus the intron segment becomes recognized as an exon during the splicing process. Therefore, the decision tree should categorize these pathological exons as authentic exons. Remarkably, all nine pathological exons were correctly categorized into one of the four exon groups: four in group A, three in group C, and one in each of groups D and E. Therefore, we consider our decision tree a suitable classifier of pathological *dystrophin* exons.

Seven indexes were used in common by both the preliminary and re-constructed trees. However, their values in each tree were different, except for one (≤ 1.39 ME3'ss score at the first node). When we compared the two trees, we found that three exons (2, 70, and 78) and two exons (40 and 56) were re-categorized into small groups (groups E and D) and the largest group (group C), respectively. This indicated slight changes in the categorizing pathways between the two trees. The cryptic exons were ultimately categorized into four groups, and exon 11a belonged to group d, which comprises exons 1a, 2a, and 3a-l. It was interesting that group D was categorized by a SIZE score of ≤ 114 (Figure 3). This indicates that a small exon can be real if the splicing silencer density is high.

Among the 26 indexes used as candidates for the decision markers, only eight were used in the tree. Furthermore, five

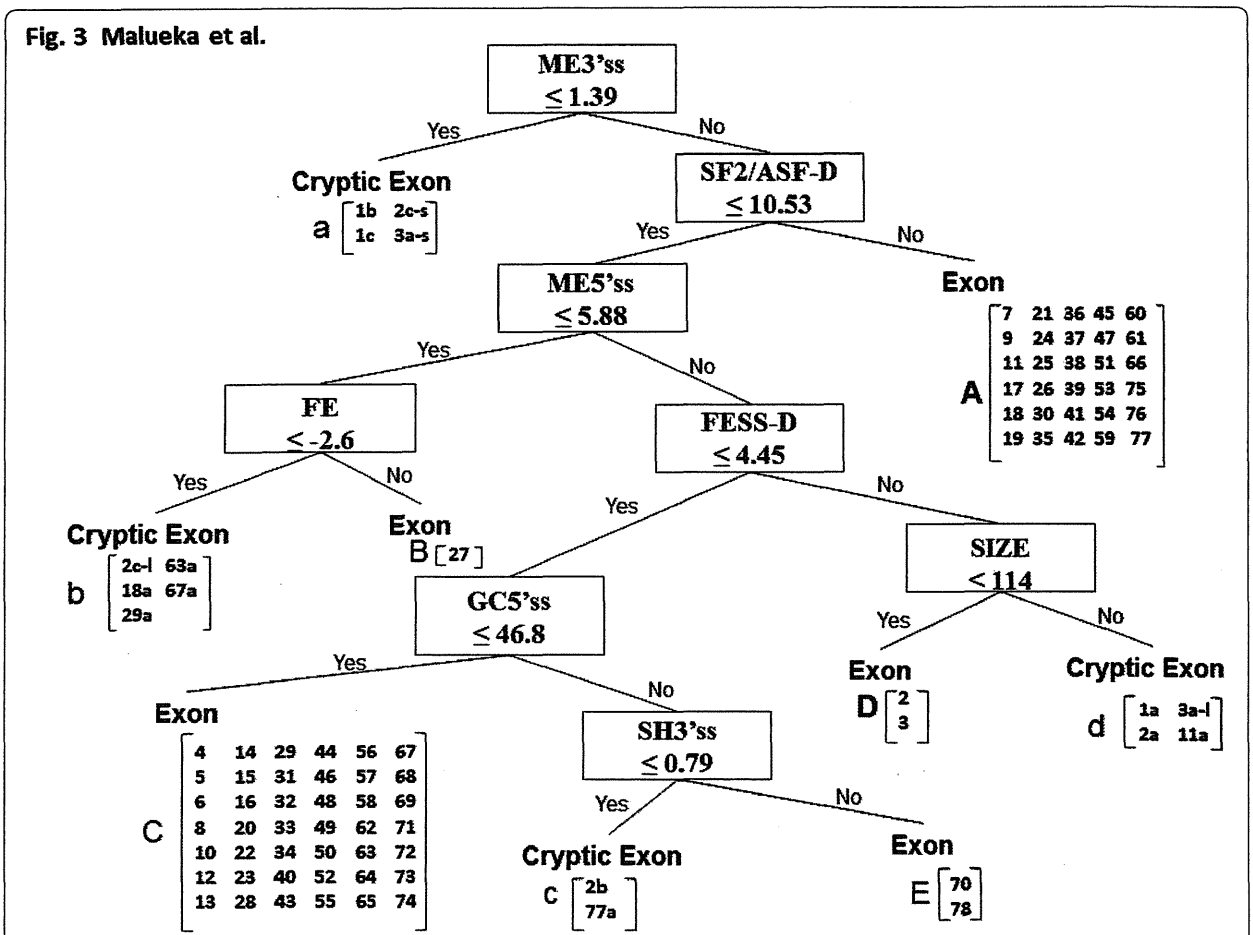

Figure 3 Final decision tree to classify 77 authentic and 15 cryptic *dystrophin* exons. The structure of the tree is as described for Figure 1. The features tested in this tree include seven indexes used in the preliminary tree (Figure 1) and one additional index, exon size (SIZE). This tree classified the authentic *dystrophin* exons into five groups (groups A to E), containing 30, 1, 42, 2, and 2 exons, respectively. The cryptic exons were classified into four groups (groups a to d).

of these eight were those determining the strength of splice sites (Table 1). This indicates that recognition of the splicing sites is very important for proper splicing. Group E (exons 70 and 78) was categorized through six nodes; the final one discriminating it from group c (cryptic exons 2b and 77a). For this categorization, the strength of the 3'ss was tested twice using different indexes (ME3'ss and SH3'ss). This indicates the importance of the 3'ss strength relative to the 5'ss strength in *dystrophin* splicing. Indexes of ESE density (SF2/ASF-D) and ESS density (FESS-D) were also used in the tree. This indicates that both the ESE and ESS densities are important in the splicing process.

Next, we used the tree to characterize exons that are subjected to specific splicing patterns. First, we marked exons known to be alternatively spliced (data not shown). However, they were found in all five groups. This indicates that no particular *cis*-elements predispose to alternative splicing. Second, we examined exons that were prone to splicing errors caused by intra-exon mutation. We have previously reported nonsense mutation-induced exon skipping in seven exons (exons 14, 15, 17, 27, 41, 42, and 70) [16]. Among these, only four (exons 17, 27, 41, and 42) cause disruption of an ESE. Remarkably, exons 17, 41, and 42 were categorized in group A, while all those that do not disrupt an ESE were categorized in other groups. This indicates that, for exons in group A, nonsense mutation-induced exon skipping is caused by disruption of an ESE, while for exons in other groups, nonsense mutation-induced exon skipping is caused by other factors. Third, we examined exons that splice to tissue-specific exon 1 (exons 2, 30, 45, 56, and 63). We did not identify any particular categorization characteristics for these exons.

Discussion

The *dystrophin* gene produces many mRNAs because it is so complex: it contains 79 exons, huge introns, eight

Table 1 Summary of categorization of exons by the decision tree

		Number of Exon	Indexes							
			ME3'ss	SF2/ASF-D	ME5'SS	FE	FESS-D	GC5'ss	SH3'ss	SIZE
Group	A	30	H	H	-	-	-	-	-	-
	B	1	H	L	L	H	-	-	-	-
	C	42	H	L	H	-	L	L	-	-
	D	2	H	L	H	-	H	-	-	L
	E	2	H	L	H	-	L	H	H	-

Results of categorization of 77 *dystrophin* exons are tabulated. Indexes determining the strength of splice sites are marked bold. H and L represent high and low at each node, respectively. Bars indicate not applicable.

tissue-specific promoters, 15 cryptic exons, and generates many alternatively spliced products. It has been reported that there is a gradient in exon and intron definition at the level of pre-mRNA splicing [17]. For example, efficient use of intrinsically weak cryptic splice sites in exons is facilitated by a higher-than-average density of ESSs and a high density of SF2/ASF ESE motifs [17]. This suggests that each exon has a specific splicing regulatory mechanism in which particular splicing factors could compensate for the lack of other splicing factors. It is important to understand more about the splicing regulatory mechanisms for each exon of the *dystrophin* gene because treatment with exon skipping is a promising therapeutic approach.

Decision trees have been used in many kinds of classifications, such as for the management of Parkinson's disease, disease severity profiling, large-scale proteomic studies, and microarray data classification [14,18]. Here, we classified 77 authentic and 15 cryptic *dystrophin* exons into five groups based on their splicing regulatory factor characteristics. In this study, we needed to modify our preliminary decision tree (Figure 1) based on data from the novel exon 11a (Figure 2). This suggested a possibility that the tree needs further modification when another cryptic exon is identified in the future construction. However, we believe any modifications, if necessary, will be minimal as exon 11a was additionally analyzed (Figure 3). Moreover, our trees were constructed using indexes obtained only from *cis*-elements; further modification incorporating information from *trans*-elements may further improve the reliability of the tree.

We used our decision tree to determine the parameters that are most useful for the discrimination of authentic and cryptic *dystrophin* exons. We separated the two categories completely using eight variables: (1) strength of the 3'ss measured by maximum entropy score; (2) density of ESEs particularly SF2/ASF; (3) strength of the 5'ss measured by maximum entropy score; (4) free energy in U1-snRNP binding to the 5'ss; (5) density of ESSs as identified by FESS-D; (6) GC content at the 5'ss; (7) exon size; and (8) strength of the 3'ss as measured by the Shapiro score. In other words, the strength of the 3'ss consensus sequence as indicated by maximum entropy score is the most critical, as all authentic *dystrophin* exons must have a maximum entropy score of more than 1.39 at the 3'ss. The next most important deciding factor is ESE density, particularly for SF2/ASF; almost half (30) of *dystrophin* exons can be classified based on this parameter and 3'ss strength only. These findings are in line with those of a previous report, which showed that exons that are skipped because of splice site mutations have a weaker 3'ss and a lower-than-average density of ESEs [17].

Our exon categorization suggested that there are at least five different patterns of splicing regulatory mechanisms for *dystrophin* pre-mRNAs (Table 1). At the extreme, one group contained only one exon (exon 27; group B), implying that this exon has a unique splicing regulatory mechanism. In fact, alteration of exon 27 splicing has been reported for two nonsense mutations, resulting in a mild phenotype [19]. Exon 27 may be particularly vulnerable to splicing alterations caused by intra-exonic mutations.

On the other hand, two groups (A and C) contained 72 out of 77 exons, suggesting that most *dystrophin* exons are under similar splicing control. Group A, consisting of 32 exons, was characterized by a high density of ESEs, particularly SF2/ASF (more than 10.53) (Figure 3) (Table 1), indicating that ESE density plays a critical role in the splicing of these exons. Disruption of ESEs for exons in this group is more likely to cause exon skipping compared with disruption of ESEs in the other exon groups. Nonsense mutations within exons 17, 41, and 42, all belonging to group A, have been shown to induce exon skipping [16]. Accordingly, the nonsense mutations in these three exons disrupt an ESE sequence and thus cause exon skipping, while nonsense mutations that induce skipping of exons in other groups do not disrupt an ESE [16]. However, not all ESE-disrupting nonsense mutations identified in these exons induce exon skipping [16]. It may be necessary to consider *trans*-elements to explain these differences, along with the strength of splicing factor binding to the ESEs and their positions in the pre-mRNA secondary structure.

Intronic pseudo-exons that look like perfect exons, maintaining splicing consensus sequences, are now under intensive investigation [10,20-22]. There is

evidence that inclusion of many of these sequences in mRNAs is actively inhibited because of the presence of intrinsic defects, the presence of silencer elements, or the formation of an inhibitory RNA secondary structure [23]. We categorized the cryptic exons into four groups (Figure 3), indicating a heterogeneous contribution of splicing factors required for their activation.

Group C contained 42 exons and was separated at the fifth node by a score of less than 46.8% GC content at the 5'ss. More than half of the *dystrophin* exons belonged to this group and are therefore presumed to be subject to similar splicing regulation. From the decision tree we can see that this group is characterized also by an ESS density ≤ 4.45 (FESS-D), indicating that splicing silencer signals play a critical role in the splicing of these exons. Indeed, we showed previously that nonsense mutation-induced exon skipping of exon 31 was caused by the creation of a splicing silencer-binding site for hnRNP A1 [13]. It has been reported that negative elements play important roles in distinguishing real splicing signals from the vast number of false-positive splicing signals [9].

Because the *dystrophin* gene is so complex, it has the potential to produce many alternatively spliced transcripts that are translated into protein variants [24]. However, studies on alternative splicing are limited [6-8]. In one study, Sironi et al. identified 16 alternative transcripts and examined splicing regulatory factors such as the 3' and 5' consensus values and exonic splicing enhancer scoring matrices; however, no reasonable explanation of the alternative splicing was identified [7]. This is consistent with our findings that the cryptic exons fell into five different groups. It is possible that alternative splicing does not rely completely on specific sequence elements and is regulated by *trans*-acting factors.

Interest in the splicing regulation of *dystrophin* pre-mRNA was first aroused when exon skipping caused by a small intra-exonic deletion was identified in a DMD patient [25]. Subsequently it was revealed that the deleted region was an ESE sequence within exon 19 [1] and that AOs against this ESE successfully induced the skipping of exon 19 [26]. This has led to the establishment of exon-skipping therapy [27]. In this study, we demonstrated that exon 19 was categorized into group A, characterized by a high ESE density; hence it is reasonable that AOs against the exon 19 ESE would induce exon skipping efficiently. Currently exon skipping is recognized as the most promising way to express dystrophin in DMD. The main targets for exon skipping therapy are exons 44, 45, 51, and 53 [28] and AOs against exon 51 are now in phase II or III clinical trials [2,3]. Because exons 45, 51, and 53 belong to group A, we would expect AOs against the ESEs in these exons to work well.

Conclusions

The decision tree categorized the 77 authentic *dystrophin* exons into five groups. Our classification may help to establish the strategy for exon skipping therapy for DMD.

Methods

Indexes of splicing regulatory factors

The sequences of 14 known cryptic exons, and nine disease-causing mutations were obtained from our previous report [10] and the literature [29,30]. Twenty six indexes of splicing regulatory factors of each exon were obtained as described below (Table 2).

Splice site strength

Splice site strength was determined in three ways: Shapiro's splicing probability matrix scores at the 5'ss and the 3'ss were calculated using published formulae [17,31] (SH5'ss and SH3'ss, respectively). Maximum entropy scores at the 5'ss and the 3'ss were obtained using online tools available at http://genes.mit.edu/burgelab/maxent/Xmaxentscan_scoreseq.html (ME5'ss and ME3'ss, respectively) [32]. Information content values at the 5'ss and the 3'ss were obtained using the Delila server at https://splice.uwo.ca/ (Ri5'ss and Ri3'ss, respectively) [33].

Free energy of U1 snRNA binding to the 5'ss

U1 snRNA binding to constitutive splice sites has lower free energy than that of its binding to alternatively spliced exon splice sites [34]. Free energy was analyzed using the SROOGLE server at http://sroogle.tau.ac.il/ (FE) [35].

Numbers and densities of ESEs and ESSs

The number of ESEs in each exon was calculated using the prediction algorithm at http://genes.mit.edu/burgelab/rescue-ese/ (RESE). The number of ESSs was calculated using two algorithms: at http://genes.mit.edu/fas-ess/ (FESS) and http://cubweb.biology.columbia.edu/pesx/ (PESS) [17,36-38]. To calculate the densities of ESSs/ESEs, the RESE, FESS, and PESS numbers were divided by the sequence length (in nucleotides) and this figure was multiplied by 100 [17] to give the RESE-D, FESS-D, and PESS-D scores.

The numbers of binding sites for the four SR proteins (SF2/ASF, SRp40, SC35, and SRp55) were obtained using ESEfinder (v. 3.0) available at http://rulai.cshl.edu/cgi-bin/tools/ESE3/esefinder.cgi?process=home (SF2/ASF-N, SRp40-N, SC35-N, and SRp55-N) [39]. The density of SR protein-binding sites (SF2/ASF-D, SC35-D, SRp40-D, SRp55-D) was obtained by dividing each number by its nucleotide length then multiplying it by 100 [17].

Minimum free energy value of pre-mRNA secondary structure and GC content around splice sites

Minimum free energy values of the pre-mRNA secondary structure at the 5'ss and 3'ss were obtained using the free energy minimization program RNAfold http://rna.tbi.univie.ac.at/cgi-bin/RNAfold.cgi using the 70

Table 2 Indexes of splicing regulatory factors

No	Features	Symbol	Reference
1	5' splice site strength (Shapiro score)	SH5'ss	[31]
2	3' splice site strength (Shapiro score)	SH3'ss	[31]
3	5' spice site strength (maximum entropy)	ME5'ss	[32]
4	3' spice site strength (maximum entropy)	ME3'ss	[32]
5	5' splice site strength (information content/Ri)	Ri5'ss	[33]
6	3' splice site strength (information content/Ri)	Ri3'ss	[33]
7	U1 SnRNA binding free energy	FE	[35]
8	ESE density (RESCUE ESE/RESE)	RESE-D	[36]
9	ESE density (PESE)	PESE-D	[38]
10	ESS density (FAS-ESS/FESS)	FESS-D	[37]
11	ESS density (PESS)	PESS-D	[38]
12	SF2/ASF number	SF2/ASF-N	[39]
13	SF2/ASF (IgM/BRCA1) number	SF2/ASF (IgM, BRCA1)-N	[39]
14	SRp40 number	SRp40-N	[39]
15	SC35 number	SC35-N	[39]
16	SRp55 number	SRp55-N	[39]
17	SF2/ASF score density	SF2/ASF-D	[39]
18	SF2/ASF (IgM/BRCA1) score density	SF2/ASF (IgM-BRCA1)-D	[39]
19	SC35 score density	SC35-D	[39]
20	SRp40 score density	SRp40-D	[39]
21	SRp55 score density	SRp55-D	[39]
22	5' splice site pre-mRNA secondary structure free energy	RSS5'ss	[40]
23	3' splice site pre-mRNA secondary structure free energy	RSS3'ss	[40]
24	5' splice site GC content	GC5'ss	[40]
25	3' splice site GC content	GC3'ss	[40]
26	The number of nucleotides in exon	SIZE	

nucleotides both up- and down-stream of each splice site (RSS5'ss and RSS3'ss, respectively) [40,41].

GC content around splice sites has been reported to affect splicing [40]. Thus, the percentage of GC content for each 70 nucleotides both up- and down-stream of the 5'ss and the 3'ss was calculated (GC5'ss and GC3'ss, respectively) [40].

Exon size

The number of nucleotides in each exon was also taken into account (SIZE).

Construction of decision trees

The C4.5 algorithm was used to construct decision trees. The C4.5 decision tree algorithm is an approach for pattern recognition and data mining [42,43] and was developed by Quinlan [44,45]. The algorithm uses information gain, which is an entropy-based criterion in information theory for decision tree construction. In this study, the conditions were as follows: (1) at least one object was to be contained in each branch, (2) the pruning confidence level was set to 100%, and (3) the iterative mode was used to avoid a local optimum.

We used 92 out of 94 data points (79 exons and 15 cryptic exons) for decision tree construction. We excluded two exons, exons 1 and 79, because they lacked some feature values.

Dystrophin mRNA analysis

A 1-year-old Japanese boy (KUCG 952) without any family history of neuromuscular disorders was referred to Kobe University Hospital (Kobe, Japan) because of a high serum creatine kinase level (37,110 IU/l). DMD was tentatively diagnosed, and mutation in the *dystrophin* gene was analyzed after obtaining informed consent from his parents. *Dystrophin* mRNA expressed in his peripheral lymphocytes was analyzed as described previously [10,25]. A fragment spanning exons 10 to 14 was amplified by reverse transcription (RT)-nested PCR using two sets of primers. The outer primer set comprised a forward primer, 1A 5'-TTTTTATCGCTGCCTTGATATACA-3' and a reverse primer, 1B 5'-ACTCTGCAACACAGCTTCTGAG-3'; the inner primer set comprised a forward primer, 1E 5'-TTGCAAGCACAAGGAGAGATT-3' and a reverse primer, c14r 5'-ACGTTGCCATTTGAGAAGGAT-3'. The

amplified fragments were resolved by agarose gel electrophoresis. Sequencing of the amplified products was performed by subcloning sequencing as described previously [46].

The mutation study was approved by our ethical committee and mutation analysis of the *dystrophin* gene was done after obtaining the informed consent from the parents of the patient.

Abbreviations

DMD: Duchenne muscular dystrophy; AO: Antisense oligonucleotide; ESE: Exonic splicing enhancer; ESS: Exonic splicing silencer; ME3'ss: Maximum entropy of 3' splice site; SF2/ASF-D: SF2/ASF score density; ME5'SS: Maximum entropy of 5' splice site; FE: Free energy of U1 SnRNA binding; FESS-D: Fluorescence-activated screen-for exonic splicing silencers density; GC5'ss: GC content of 5' splice site; SH3'ss: Shapiro score of 3' splice site; SIZE: Size of exon.

Acknowledgements

This work was supported by a Grant-in-Aid for Scientific Research (B), and a Grant-in-Aid for Exploratory Research from the Japan Society for the Promotion of Science, a Health and Labour Sciences Research Grant for Research on Psychiatric and Neurological Diseases and Mental Health, and a research grant for Nervous and Mental Disorders from the Ministry of Health, Labour and Welfare, Japan.

Author details

[1]Department of Pediatrics, Graduate School of Medicine, Kobe University, Chuo, Kobe 6500017, Japan. [2]Division of Medical Informatics and Bioinformatics, Kobe University Hospital, Chuo, Kobe 6500017, Japan. [3]Department of Clinical Pharmacy, Kobe Pharmaceutical University, Higashinada, Kobe 6588558, Japan. [4]Department of Medical Rehabilitation, Faculty of Rehabilitation, Kobegakuin University, 518 Arise, Ikawadani, Nishi, Kobe 651-2180, Japan.

Authors' contributions

RGM carried out the molecular genetic studies, participated in the bioinformatics analysis and drafted the manuscript. YT carried out the bioinformatics analysis. MY, HA, TL and EKD participated in the clinical and genetic analysis. YT participated in the design of the study. MM conceived of the study, and participated in its design and coordination and helped to draft the manuscript. All authors read and approved the final manuscript.

Competing interests

The authors declare that they have no competing interests.

Received: 18 January 2012 Accepted: 31 March 2012
Published: 31 March 2012

References

1. Takeshima Y, Nishio H, Sakamoto H, Nakamura H, Matsuo M: **Modulation of in vitro splicing of the upstream intron by modifying an intra-exon sequence which is deleted from the *dystrophin* gene in *dystrophin* Kobe.** *J Clin Invest* 1995, **95**:515-520.
2. Aartsma-Rus A: **Antisense-mediated modulation of splicing: Therapeutic implications for duchenne muscular dystrophy.** *RNA Biol* 2010, **7(4)**:453-461.
3. Lu QL, Yokota T, Takeda S, Garcia L, Muntoni F, Partridge T: **The Status of Exon Skipping as a Therapeutic Approach to Duchenne Muscular Dystrophy.** *Mol Ther* 2011, **19**:9-15.
4. Ahn AH, Kunkel LM: **The structural and functional diversity of *dystrophin*.** *Nat Genet* 1993, **3**:283-291.
5. Nishio H, Takeshima Y, Narita N, Yanagawa H, Suzuki Y, Ishikawa Y, Minami R, Nakamura H, Matsuo M: **Identification of a novel first exon in the human *dystrophin* gene and of a new promoter located more than 500 kb upstream of the nearest known promoter.** *J Clin Invest* 1994, **94**:1037-1042.
6. Feener CA, Koenig M, Kunkel LM: **Alternative splicing of human *dystrophin* mRNA generates isoforms at the carboxy terminus.** *Nature* 1989, **338**:509-511.
7. Sironi M, Cagliani R, Pozzoli U, Bardoni A, Comi GP, Giorda R, Bresolin N: **The *dystrophin* gene is alternatively spliced throughout its coding sequence.** *FEBS Lett* 2002, **517**:163-166.
8. Kubokawa I, Takeshima Y, Ota M, Enomoto M, Okizuka Y, Mori T, Nishimura N, Awano H, Yagi M, Matsuo M: **Molecular characterization of the 5'-UTR of retinal *dystrophin* reveals a cryptic intron that regulates translational activity.** *Mol Vis* 2010, **16**:2590-2597.
9. Sun H, Chasin LA: **Multiple splicing defects in an intronic false exon.** *Mol Cell Biol* 2000, **20**:6414-6425.
10. Zhang Z, Habara Y, Nishiyama A, Oyazato Y, Yagi M, Takeshima Y, Matsuo M: **Identification of seven novel cryptic exons embedded in the *dystrophin* gene and characterization of 14 cryptic *dystrophin* exons.** *J Hum Genet* 2007, **52**:607-617.
11. Valadkhan S: **Role of the snRNAs in spliceosomal active site.** *RNA Biol* 2010, **7**:345-353.
12. Matlin AJ, Clark F, Smith CW: **Understanding alternative splicing: towards a cellular code.** *Nat Rev Mol Cell Biol* 2005, **6**:386-398.
13. Nishida A, Kataoka N, Takeshima Y, Yagi M, Awano H, Ota M, Itoh K, Hagiwara M, Matsuo M: **Chemical treatment enhances skipping of a mutated exon in the *dystrophin* gene.** *Nat Commun* 2011, **2**:308.
14. Kingsford C, Salzberg SL: **What are decision trees?** *Nat Biotechnol* 2008, **26**:1011-1013.
15. Allen JE, Majoros WH, Pertea M, Salzberg SL: **JIGSAW, GeneZilla, and GlimmerHMM: puzzling out the features of human genes in the ENCODE regions.** *Genome Biol* 2006, **7(Suppl 1:S9)**:1-13.
16. Nishiyama A, Takeshima Y, Zhang Z, Habara Y, Tran TH, Yagi M, Matsuo M: ***Dystrophin* nonsense mutations can generate alternative rescue transcripts in lymphocytes.** *Ann Hum Genet* 2008, **72**:717-724.
17. Královicová J, Vorechovsky I: **Global control of aberrant splice-site activation by auxiliary splicing sequences: evidence for a gradient in exon and intron definition.** *Nucleic Acids Res* 2007, **35**:6399-6413.
18. David MP, Concepcion GP, Padlan EA: **Using simple artificial intelligence methods for predicting amyloidogenesis in antibodies.** *BMC Bioinforma* 2010, **11**:79.
19. Shiga N, Takeshima Y, Sakamoto H, Inoue K, Yokota Y, Yokoyama M, Matsuo M: **Disruption of the splicing enhancer sequence within exon 27 of the *dystrophin* gene by a nonsense mutation induces partial skipping of the exon and is responsible for Becker muscular dystrophy.** *J Clin Invest* 1997, **100**:2204-2210.
20. Buratti E, Chivers M, Královicová J, Romano M, Baralle M, Krainer A, Vorechovsky I: **Aberrant 5' splice sites in human disease genes: mutation pattern, nucleotide structure and comparison of computational tools that predict their utilization.** *Nucleic Acids Res* 2007, **35**:4250-4263.
21. Dhir A, Buratti E: **Alternative splicing: role of pseudoexons in human disease and potential therapeutic strategies.** *FEBS J* 2010, **277**:841-855.
22. Vorechovsky I: **Transposable elements in disease-associated cryptic exons.** *Hum Genet* 2010, **127**:135-154.
23. Dhir A, Buratti E, van Santen MA, Luhrmann R, Baralle FE: **The intronic splicing code: multiple factors involved in ATM pseudoexon definition.** *EMBO J* 2010, **29**:749-760.
24. Wei B, Jin JP: **Troponin T isoforms and posttranscriptional modifications: Evolution, regulation and function.** *Arch Biochem Biophys* 2011, **505**:144-154.
25. Matsuo M, Masumura T, Nishio H, Nakajima T, Kitoh Y, Takumi T, Koga J, Nakamura H: **Exon skipping during splicing of *dystrophin* mRNA precursor due to an intraexon deletion in the *dystrophin* gene of Duchenne muscular dystrophy Kobe.** *J Clin Invest* 1991, **87**:2127-2131.
26. Pramono ZA, Takeshima Y, Alimsardjono H, Ishii A, Takeda S, Matsuo M: **Induction of exon skipping of the *dystrophin* transcript in lymphoblastoid cells by transfecting an antisense oligodeoxynucleotide complementary to an exon recognition sequence.** *Biochem Biophys Res Commun* 1996, **226**:445-449.
27. Takeshima Y, Yagi M, Wada H, Ishibashi K, Nishiyama A, Kakumoto M, Sakaeda T, Saura R, Okumura K, Matsuo M: **Intravenous infusion of an antisense oligonucleotide results in exon skipping in muscle *dystrophin* mRNA of Duchenne muscular dystrophy.** *Pediatr Res* 2006, **59**:690-694.
28. Takeshima Y, Yagi M, Okizuka Y, Awano H, Zhang Z, Yamauchi Y, Nishio H, Matsuo M: **Mutation spectrum of the *dystrophin* gene in 442 Duchenne/**

Becker muscular dystrophy cases from one Japanese referral center. *J Hum Genet* 2010, **55**:379-388.
29. Yagi M, Takeshima Y, Wada H, Nakamura H, Matsuo M: **Two alternative exons can result from activation of the cryptic splice acceptor site deep within intron 2 of the *dystrophin* gene in a patient with as yet asymptomatic dystrophinopathy.** *Hum Genet* 2003, **112**:164-170.
30. Beroud C, Carrie A, Beldjord C, Deburgrave N, Llense S, Carelle N, Peccate C, Cuisset JM, Pandit F, Carre-Pigeon F, *et al*: **Dystrophinopathy caused by mid-intronic substitutions activating cryptic exons in the DMD gene.** *Neuromuscul Disord* 2004, **14**:10-18.
31. Shapiro MB, Senapathy P: **RNA splice junctions of different classes of eukaryotes: sequence statistics and functional implications in gene expression.** *Nucleic Acids Res* 1987, **15**:7155-7174.
32. Yeo G, Burge CB: **Maximum entrophy modeling of short sequence motifs with applications to RNA splicing signals.** *J Comput Biol* 2003, **11**:377-394.
33. Nalla VK, Rogan PK: **Automated splicing mutation analysis by information theory.** *Hum Mutat* 2005, **25**:334-342.
34. Ast G: **How did alternative splicing evolve?** *Nat Rev Genet* 2004, **5**:773-782.
35. Schwartz S, Hall E, Ast G: **SROOGLE: webserver for integrative, user-friendly visualization of splicing signals.** *Nucleic Acids Res* 2009, **37(Web Server)**:W189-192.
36. Fairbrother WG, Yeh RF, Sharp PA, Burge CB: **Predictive identification of exonic splicing enhancers in human genes.** *Science* 2002, **297**:1007-1013.
37. Wang Z, Rolish ME, Yeo G, Tung V, Mawson M, Burge CB: **Systematic identification and analysis of exonic splicing silencers.** *Cell* 2004, **119**:831-845.
38. Zhang XH, Chasin LA: **Computational definition of sequence motifs governing constitutive exon splicing.** *Genes Dev* 2004, **18**:1241-1250.
39. Cartegni L, Wang J, Zhu Z, Zhang MQ, Krainer AR: **ESEfinder: A web resource to identify exonic splicing enhancers.** *Nucleic Acids Res* 2003, **31**:3568-3571.
40. Zhang J, Kuo CC, Chen L: **GC content around splice sites affects splicing through pre-mRNA secondary structures.** *BMC Genomics* 2011, **12**:90.
41. Gruber AR, Lorenz R, Bernhart SH, Neubock R, Hofacker IL: **The Vienna RNA websuite.** *Nucleic Acids Res* 2008, **36(Web Server)**:W70-74.
42. Han J, Kamber M, Pei J: *Data Mining: Concepts and Techniques* Waltham, Massachusetts: Morgan Kaufmann Publishers; 2011.
43. Witten IH, Frank E: *Practical Machine Learning Tools and Techniques* Waltham, Massachusetts: Morgan Kaufmann Publishers; 2005.
44. Quinlan JR: *C4.5: Programs for Machine Learning* Waltham, Massachusetts: Morgan Kaufmann Publishers; 1993.
45. Quinlan JR: **Improved Use of Continuous Attributes in C.** *J Artif Intell Res* 1996, **4**:77-90.
46. Surono A, Takeshima Y, Wibawa T, Ikezawa M, Nonaka I, Matsuo M: **Circular *dystrophin* RNAs consisting of exons that were skipped by alternative splicing.** *Hum Mol Genet* 1999, **8**:493-500.

doi:10.1186/1471-2156-13-23
Cite this article as: Malueka *et al.*: Categorization of 77 *dystrophin* exons into 5 groups by a decision tree using indexes of splicing regulatory factors as decision markers. *BMC Genetics* 2012 **13**:23.

NUCLEIC ACID THERAPEUTICS
Volume 21, Number 5, 2011

DOI: 10.1089/nat.2011.0310

Antisense Oligonucleotide Induced *Dystrophin* Exon 45 Skipping at a Low Half-Maximal Effective Concentration in a Cell-Free Splicing System

Rusdy Ghazali Malueka,[1] Mariko Yagi,[1] Hiroyuki Awano,[1] Tomoko Lee,[1] Ery Kus Dwianingsih,[1] Atsushi Nishida,[1,2] Yasuhiro Takeshima,[1] and Masafumi Matsuo[1,3]

Antisense oligonucleotides (AOs) can facilitate the expression of internally deleted dystrophin in dystrophin-deficient Duchenne muscular dystrophy (DMD) by correcting the reading frame of the pre-mRNA with AO-mediated exon skipping. An antisense 18-mer 2′-O-methyl RNA/ethylene-bridged nucleic acid chimera AO targeting exon 45 of the *dystrophin* gene, *AO85*, can induce exon 45 skipping efficiently in cultured cells. AO85 is expected to facilitate dystrophin expression in 8%–9% of all DMD patients. Here, we examined the kinetics of AO85-mediated exon 45 skipping in a cell-free splicing system. *In vitro* transcribed pre-mRNAs containing *dystrophin* exon 45 and part of its flanking introns within a hybrid minigene were incubated with HeLa cell nuclear extract, and the resultant mRNAs were amplified by semiquantitative reverse transcriptase–polymerase chain reaction. Time-course analysis revealed that the splicing process fitted well to first order kinetics. Addition of AO85 produced an extra spliced product, deleting exon 45 (Δexon 45), indicating AO85-mediated exon 45 skipping. Production of Δexon 45 increased linearly with increasing concentrations of AO85, reaching a maximum of nearly 80% of the transcripts. The half-maximal effective concentration (EC_{50}) of AO85 was 58.0 nM. The percentage of Δexon 45 among the transcripts decreased inversely with the pre-mRNA concentration; Lineweaver-Burk plotting revealed a competitive fashion of AO85 action. The low EC_{50} indicates high potential of AO85 for clinical application.

Introduction

ANTISENSE OLIGONUCLEOTIDES (AOs) are traditionally employed to destroy the target RNA by RNAase H-mediated digestion (Pan and Clawson, 2006). AO action is dependent on binding to specific mRNA sequences through Watson-Crick base pair hybridization, before digestion of the bound fragment by RNAase H. AOs have been applied to the treatment of infectious diseases or cancers by degrading target mRNAs (Van Aerschot, 2006; Bennett and Swayze, 2010), and their kinetics have been studied (Duan et al., 2008). Currently, AOs are attracting much attention as modulators of splicing that can generate new gene transcripts (Perez et al., 2010; Wood et al., 2010).

Duchenne muscular dystrophy (DMD) is a rapidly progressive muscle wasting disease that usually results in death during the third decade. DMD is characterized by a dystrophin deficiency that usually arises from out-of-frame deletion mutations in the *dystrophin* gene that create a premature stop codon in the *dystrophin* mRNA. AO-mediated exon skipping therapy has been proposed for the treatment of DMD, producing in-frame *dystrophin* mRNA from the out-of-frame mRNA by inducing exon skipping. The newly generated in-frame *dystrophin* mRNA is expected to produce semifunctional, internally deleted dystrophin protein (Takeshima et al., 1995). The production of internally deleted dystrophin has been clinically demonstrated in some patients who showed natural skipping of an exon encoding a nonsense mutation (Shiga et al., 1997; Flanigan et al., 2011). Compared with gene replacement therapy, the benefits of exon skipping with AOs include the ability to use the endogenous gene and easy chemical synthesis of AOs. Currently, induction of exon skipping with AOs is considered one of the most plausible treatments for DMD (Aartsma-Rus, 2010; Lu et al., 2011). Remarkably, systemic administration of 2′-O-methyl phosphorothioate AO (PRO051) showed a promising result of a modest improvement in the 6 minutes walk test after 12 weeks of the treatment (Goemans et al., 2011).

[1]Department of Pediatrics, Graduate School of Medicine, Kobe University, Kobe, Japan.
[2]Department of Clinical Pharmacy, Kobe Pharmaceutical University, Kobe, Japan.
[3]Department of Medical Rehabilitation, Faculty of Rehabilitation, Kobegakuin University, Kobe, Japan.

AOs with phosphorothioate backbones directed against the splicing enhancer sequence within human *dystrophin* exon 19 provided the first demonstration of exon skipping in human cells (Pramono et al., 1996). Since then, intravenous infusion of AOs against exon 19 has been reported to induce exon 19 skipping and the expression of internally deleted dystrophin in an exon 20-deleted DMD patient (Takeshima et al., 2006). Several chemical modifications of the first-generation phosphorothioate AOs have been introduced over the past decade to improve the efficiency of antisense therapeutics. Morpholino AOs have been shown to induce *dystrophin* exon 51 skipping and promote dystrophin expression in DMD muscle cells (Partridge, 2010).

A modified nucleic acid, 2′-O,4′-C-ethylene-bridged nucleic acid (ENA), has high binding affinity for the complementary RNA strand and more nuclease resistance than unmodified nucleic acid (Morita et al., 2001; Veedu and Wengel, 2010). One antisense 2′-O-methyl RNA/ENA (RNA/ENA) chimera was shown to be 40 times more effective than the conventional phosphorothioate backbone oligonucleotides in inducing exon 19 skipping (Yagi et al., 2004). Furthermore, an RNA/ENA chimera against *dystrophin* exon 41 encoding a nonsense mutation has been shown to induce efficient skipping of a mutated exon 41 (Surono et al., 2004). Considering that skipping of exon 45 is expected to express internally deleted dystrophin in 8%–9% of DMD patients (Aartsma-Rus et al., 2009a; Takeshima et al., 2010), AOs that induce exon 45 skipping have been proposed as one of the most important AOs for DMD treatment. In our previous studies, we demonstrated that an 18-mer RNA/ENA chimera, AO85, strongly induced exon 45 skipping in cultured myocytes (Takagi et al., 2004a; Takeshima et al., 2011). However, its kinetics, including the half-maximal effective concentration (EC50), are still unknown, as for other AOs designed for DMD treatment (Aartsma-Rus, 2010).

To facilitate the clinical application of AO85, here we examined AO-mediated exon 45 skipping in a cell-free splicing system and determined the splicing parameters of AO85, revealing a low EC_{50}.

Materials and Methods

AO85

An 18-mer RNA/ENA chimera (5′-CgCTgcCCaaTgC-CatCC-3′; upper and lower case letters represent ENA and 2′-O-methyl RNA, respectively), AO85, complementary to the 5′ region of *dystrophin* exon 45 (Takeshima et al., 2011), was synthesized by KNC Laboratories Co. (Kobe, Japan) and dissolved in water.

In vitro *transcription*

The region encompassing *dystrophin* exon 45 and part of its flanking introns was amplified from human genomic DNA by polymerase chain reaction (PCR) using a set of primers containing *Nhe*I and *Bam*HI restriction enzyme recognition sites (forward primer, Int44F*Nhe*I 5′-GCGGCTAGCGCTA ACCGAGAGGGTGCTTTT-3′; reverse primer, Int45R*Bam*HI 5′-GCGGGATCCGCAGAAAACCACTAACTAGCCACA-3′; restriction sites underlined). The amplified product was digested with *Nhe*I and *Bam*HI (New England Biolabs, Hitchen, UK) and inserted between the 2 exons A and B of the predigested expression vector H492 (Habara et al., 2008) to generate a hybrid minigene (Fig. 1a). The sequence of the hybrid minigene was confirmed by DNA sequencing using an ABI 3130 genetic analyzer (Applied Biosystems, Foster City, CA). A region of the hybrid minigene including exon A, *dystrophin* exon 45 and exon B was PCR amplified using forward (T7(19), 5′-TAATACGACTCACTATAGG-3′) and reverse (YH304, 5′-CTCGAGCAGCCAGTTAAGTCTCTCA C-3′) primers and then purified using a MinElute PCR Purification kit (QIAGEN, Hilden, Germany). The purified template DNAs were subjected to *in vitro* transcription using an mMESSAGE mMACHINE High Yield Capped RNA Transcription kit (Ambion, Austin, TX). After treatment of the transcription product with DNase (Ambion), the resultant RNAs were purified on a G-50 Quick Spin Column (Roche Applied Science, Indianapolis, IN) and used as a substrate for the splicing reaction. The concentration and size of the

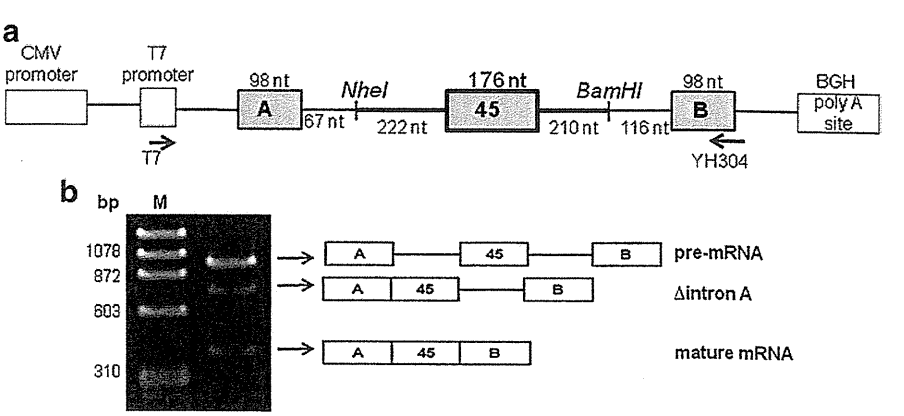

FIG. 1. Cell-free splicing reaction. **(a)** Schematic description of the hybrid-minigene. Pre-mRNA was *in vitro* transcribed from template DNA that was obtained by PCR amplification of the hybrid-minigene with primers T7 and YH304. *Shaded boxes* and *bars* indicate exons and introns, respectively. *Dystrophin* exon 45 (176 nt) and its flanking introns (222 nt upstream and 210 nt downstream; *bold lines*) were inserted into the multicloning site of the pre-constructed expression vector H492 that contains exons A and B, a cytomegalovirus (CMV) enhancer-promoter, a T7 promoter, and the bovine growth hormone gene (*BGH*) polyadenylation signal (*boxes*). **(b)** Products of the cell-free splicing reaction. The synthesized pre-mRNA was incubated with HeLa cell nuclear extract for 2 hours at 30°C. The reaction products were RT-PCR amplified and separated by agarose gel electrophoresis (indicated). The structure of each product is described schematically on the right. *Boxes* and *bars* indicate exons and introns, respectively. RT-PCR, reverse transcriptase–polymerase chain reaction.

purified RNAs were determined using an ND-1000 spectrophotometer (NanoDrop, Wilmington, DE) and an Agilent 2100 Bioanalyzer with an RNA Nano kit (Agilent Technologies, Santa Clara, CA), respectively.

In vitro *splicing reaction*

The *in vitro* splicing reaction was carried out at 30°C for 2 hours in a volume of 20 μL containing 30 ng pre-mRNA, 50% (v/v) HeLa cell nuclear extract (Lot No. 4168HNE; Computer Cell Culture Center, Mons, Belgium), 1.6 mM $MgCl_2$, 0.5 mM ATP, 20 mM creatine phosphate, and 20 U of RNaseOUT (Invitrogen, Carlsbad, CA) (Habara et al., 2008). In some experiments, the indicated amounts of AO85 were added directly to the reaction mixture. The incubation temperature or time was varied to study the temperature or time dependency of the *in vitro* splicing.

After the designated incubation time, reaction mixtures were treated with Proteinase K (Sigma-Aldrich, St. Louis, MO) and the resulting RNAs were purified by phenol–chloroform extraction and ethanol precipitation as previously described (Habara et al., 2008). Purified total RNA (750 ng) was reverse transcribed using random hexamer primers with M-MLV reverse transcriptase (Invitrogen) according to the manufacturer's protocol and then PCR amplified using a forward primer from exon A (YH307, 5′-ATTACTCGCTCA GAAGCTGTGTTGC-3′) and a reverse primer from exon B (YH308, 5′-AAGTCTCTCACTTAGCAACTGGCAG-3′) (Habara et al., 2008). PCRs were performed in a volume of 20 μL containing 4 μL of cDNA, 1× Ex Taq Buffer, 250 nM dNTPs (Takara Bio, Inc., Kyoto, Japan), 10 pmol of each primer, and 1 U of Ex Taq Polymerase (Takara Bio, Inc.). The PCR cycling conditions were as follows: initial denaturation at 94°C for 2 minutes followed by 16 cycles of denaturation at 94°C for 1 minute, annealing at 58°C for 1 minute, extension at 72°C for 2 minutes, and a final extension at 72°C for 5 minutes. PCR products were analyzed by agarose gel electrophoresis. Each amplified product was semiquantified by measuring the peak areas of capillary electrophoresis using an Agilent 2100 Bioanalyzer with a DNA1000 kit (Agilent Technologies). The sequences of all the detected bands were confirmed by subcloning and sequencing as previously described (Tran et al., 2006). As an internal standard, the glyceraldehyde 3-phosphate dehydrogenase (*GAPDH*) gene was also amplified by reverse transcriptase (RT)-PCR from cDNA, using primers spanning exons 3–6 of the *GAPDH* cDNA (Zhu et al., 2007).

The percentage of spliced products among the total transcripts was calculated by the following formula: splicing efficiency (%) = [spliced/(spliced + unspliced pre-mRNAs)] × 100 (Zheng and Baker, 2000). The percentage of the skipped exon among the total transcripts was defined as [Δexon45/(normally spliced product + Δexon45)] × 100. The ratio of normally spliced mRNA to the internal standard *GAPDH* was calculated and its relationship with the pre-mRNA was analyzed.

Statistical analysis

All analyses were performed using GraphPad Prism 5 (GraphPad Software, Inc., San Diego, CA). The mean ± standard deviation was derived from 2 or more independent experiments. Both nonlinear and linear regressions were used to determine the mechanism of AO85-induced exon 45 skipping.

Results

Cell-free splicing of pre-mRNA

Synthesized pre-mRNA was incubated with HeLa cell nuclear extract and the resulting products were analyzed by RT-PCR of total RNA extracted from the reaction mixture. Amplification of a fragment extending from exons A to B revealed 3 products on agarose gel electrophoresis (Fig. 1b). The largest product corresponded to the substrate pre-mRNA that maintained the 3 exons (exons A, 45, and B) and 2 introns (introns A and 45). The middle-sized product lacked the upstream intron A from the pre-mRNA (Δintron A), indicating a splicing intermediate. The smallest band lacked both introns (introns A and 45), corresponding to the mature mRNA. All 3 products showed the expected exon/exon junction sequences and there were no unexpected splicing products caused by cryptic splice site activation. Mature mRNA was obtained most abundantly at 30°C compared with at 37°C or 40°C (data not shown), as reported previously (Habara et al., 2009).

We then monitored the time-course of the splicing reaction by semiquantitative RT-PCR (Fig. 2a). With an incubation time of zero, only the pre-mRNA was detected. At 15 mins, Δintron A was also detected. This indicates that the 5′ intron,

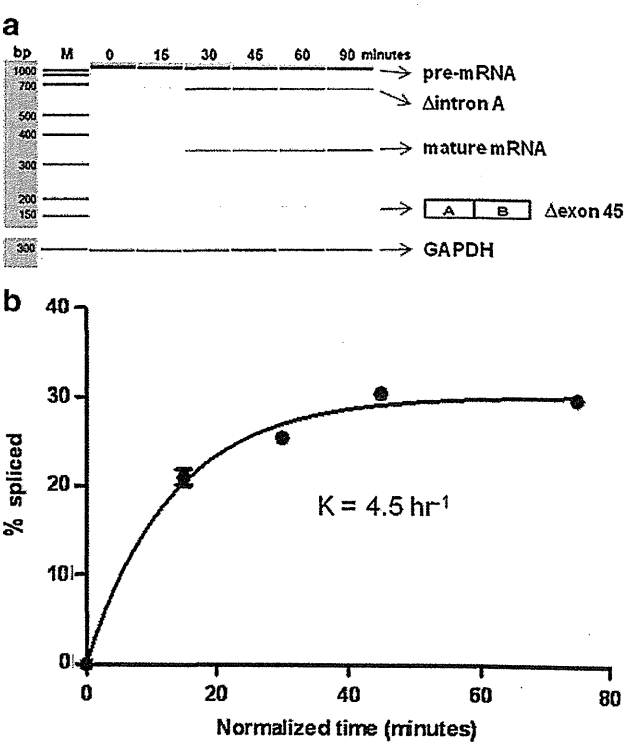

FIG. 2. Time-course of the cell-free splicing reaction. **(a)** Capillary gel electrophoretic patterns of RT-PCR products. At 15 minutes, Δintron A only was visible. From 30 minutes onwards, 3 spliced products were detected, as indicated schematically on the *right*. *Boxes* and *bars* indicate exons and introns, respectively. The *GAPDH* RT-PCR products are shown at the *bottom*. **(b)** When the 15-minute lag period was taken into consideration (corrected time), the percentage of spliced product fitted a pseudo first-order model, with a rate constant (K) of 4.5 $hour^{-1}$. Values represent the means for 3 measurements. GAPDH, glyceraldehyde 3-phosphate dehydrogenase.

intron A, was spliced first in this cell-free splicing system. At 30 minutes' incubation, the amount of Δintron A increased and the mature mRNA was detected. Trace amounts of Δexon 45 were also detected (Fig. 2a).

We then analyzed the percentage of spliced product. Because the Δintron A splicing product appeared at 15 minutes (Fig. 2a), the first 15 minutes was considered an initial lag period (Hicks et al., 2005). When the 15-min lag period was taken into consideration, the appearance of spliced products followed a profile characteristic of a first order reaction (Fig. 2b). The product appearance data fitted the pseudo-first order rate description $Y = C \times (1-e^{-kt})$, where Y is the fraction spliced, C is the fraction spliced at the end-point of the reaction, k is the apparent rate constant, and t is the time (Hicks et al., 2005). The observed rate constant was 4.5 ± 0.42 hour^{-1}, fitting well to the 1-phase association model with $R^2 = 0.9905$ (Fig. 2b) and confirming that this cell-free splicing reaction is time dependent. In the following experiments, the incubation time was shortened to 30 minutes.

Induction of exon 45 skipping with AO85

To examine whether AO85 was able to induce exon 45 skipping in the cell-free splicing system, 0–160 nM AO85 was added to the incubation mixture, and the resulting RNAs were analyzed by RT-PCR. In the absence of AO85, 3 products, corresponding to pre-mRNA, Δintron A, and mature mRNA, were clearly observed (Fig. 3a). At 20 nM AO85, the percentage of Δexon 45 increased, whereas both Δintron A and the mature mRNA decreased. At 160 nM AO85, almost 80% of the total product was Δexon 45. When the percentage of Δexon 45 was plotted against AO85 concentration, the percentage increased linearly (Fig. 3b). The data fitted well to a dose–response model, with $R^2 = 0.9990$. From this, the EC_{50} was calculated as 58.0 nM.

Competitive fashion of AO85 action

We next analyzed action patterns of AO85 in a total splicing reaction by measuring the production of mature mRNA with different concentrations of AO85 and pre-mRNA. The amount of pre-mRNA ranged from 0 to 10.5 nM with 3 different AO85 concentrations (0, 20, and 40 nM). The amount of mature mRNA was normalized to that of *GAPDH*. On a Lineweaver-Burk plot (Fig. 4a), the data showed that AO85 inhibited the production of mature mRNA in a dose-dependent manner and that 3 lines linking spots met together at the Y axis, indicating a competitive fashion of AO85 action. The *Ki* of the inhibition was found 10.1 nM (Fig. 4b).

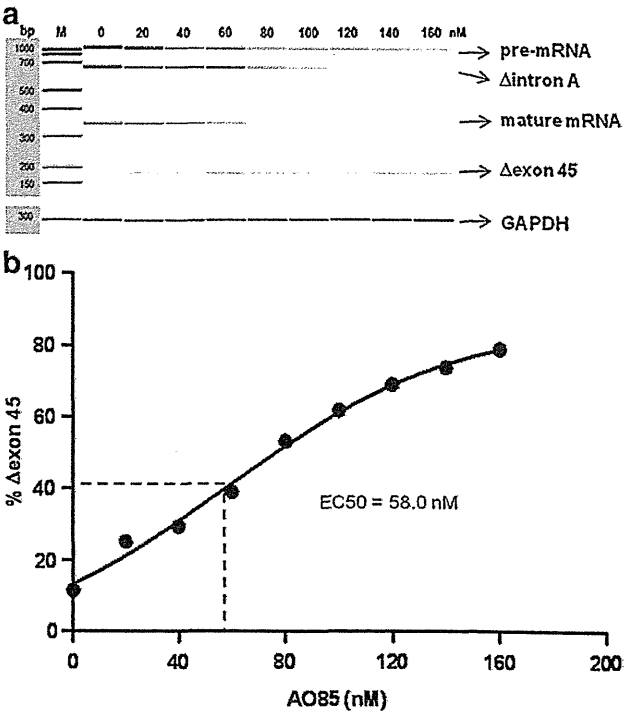

FIG. 3. Dose dependency of exon 45 skipping. **(a)** Capillary gel electrophoretic patterns of RT-PCR products. The indicated concentration (0–160 nM) of AO85 was added to the *in vitro* splicing system. The intensity of Δexon 45 increased with increasing concentration of AO85, in contrast to the intensity of the normally spliced band, as indicated schematically on the *right*. *Boxes* and *bars* indicate exons and introns, respectively. The *GAPDH* RT-PCR products are shown at the *bottom*. **(b)** The data fitted well to a linear dose–response model. The EC50 was calculated as 57.96 nM. Values represent the means for 3 measurements. AO, antisense oligonucleotide; EC50, half-maximal effective concentration.

Discussion

We showed that AO85 induced exon 45 skipping in a cell-free splicing system that contained substrate pre-mRNA and HeLa cell nuclear extract, indicating that exon skipping does not require intact cells. Regardless of the shortened introns (Fig. 1) the pre-mRNA was subjected to exon skipping. The *in vitro* splicing assay has been shown useful to examine antisense-mediated exon skipping, although there are limitations in applying the results in understanding *in vivo* splicing (Spitali et al., 2009). One of the most important limitations is that *in vitro* splicing requires the use of relatively short transcripts (approximately 1,000–2,000 bp) that usually lack the complexity and length of natural pre-mRNA, and thus may not identify the rate limiting steps for expression *in vivo* (Nasim et al., 2002). In our *in vitro* splicing system total amount of RNA decreased at the high concentration of AO85 (Fig. 3a). This may be due to tight connection of AO85 to the target sequence, hampering PCR amplification or unknown RNAse activation.

The cell-free splicing reaction had an initial lag period of up to 15 minutes (Fig. 2). Regulatory elements located within introns and exons guide the splicing complex, the spliceosome, and auxiliary RNA-binding proteins to the correct sites for intron removal and exon joining (Pandya-Jones and Black, 2009; Ward and Cooper, 2010). Presumably, exogenously added pre-mRNAs are initially coated with heteronuclear ribonucleoproteins (hnRNPs) that are abundant in nuclear extracts, and the competing association and dissociation between hnRNPs and components of the spliceosome requires time (Hicks et al., 2005). We assume that the observed lag period corresponds to the spliceosome association. After this initial phase, the splicing reaction proceeded linearly.

AO85, which was identified through trial-and-error, is considered to bind to an exon splicing enhancer (Takeshima et al., 2011). Nuclear proteins bound to the enhancer sequence

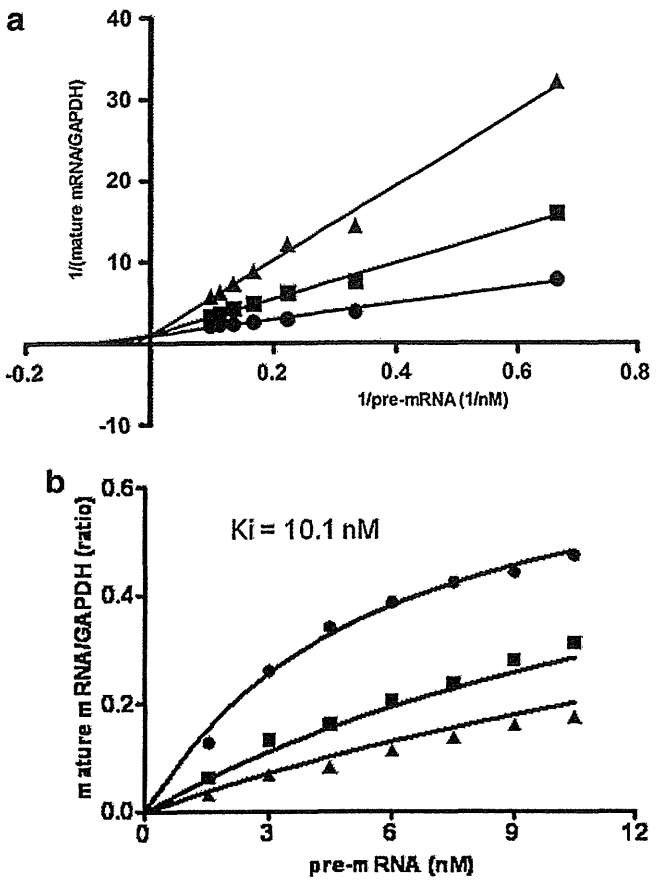

FIG. 4. Competitive fashion of of AO85 action. (a) Lineweaver-Burk plot for the production of mature mRNA for 3 concentrations of AO85 and various concentration of pre-mRNA. The ratio of normally spliced mRNA to *GAPDH* was plotted against 1/pre-mRNA concentration (0–10.5 nM). The concentrations of AO85 were 0, 20, or 40 nM (*circles*, *squares*, and *triangles*, respectively). The results showed competitive inhibition of AO85. Values represent the means of 3 experiments. (b) Nonlinear regression of production of mature mRNA in 3 concentration of AO85 and various concentration of pre-mRNA. The ratio of normally spliced mRNA was plotted against the substrate pre-mRNA concentration (0–10.5 nM). The concentration of AO85 was 0, 20, and 40 nM (*circle*, *box*, and *triangles*, respectively). The *Ki* value was calculated as 10.1 nM. Values represent means from 3 experiments.

can promote exon definition by directly recruiting other splicing factors and/or by antagonizing the action of nearby silencer elements. Thus, failure of nuclear proteins to bind to the enhancer sequence would prohibit recognition of the exon by the splicing machinery and cause exon skipping (Takeshima et al., 1995; Pramono et al., 1996; Freier and Altmann, 1997; Stahel and Zangemeister-Wittke, 2003; Aartsma-Rus et al., 2009b; Popplewell et al., 2009). AO85 is expected to bind to a region targeted by 2 SR proteins, SRp30c and SRp40 (Mathews et al., 1999), suggesting that AO85 competes with these 2 SR proteins for binding the pre-mRNA. The binding site for SRp30c is partially located where the pre-mRNA adopts an open secondary structure, whereas the predicted binding site of SRp40 is located within a closed structure (Mathews et al., 1999; Zuker, 2003). AO85 probably competes with SRp30c, but this needs further examination. Our results showing a competitive fashion of AO85 action (Fig. 4a) support the idea of competition with nuclear proteins.

Our study of the kinetics of AO85-mediated exon skipping in *in vitro* splicing revealed that (1) AO85 induced exon 45 skipping by inhibiting the production of mature mRNA, with a *Ki* of 10.1 nM. This relatively low *Ki* value indicates that AO85 is a potent competitor in the recognition of exon 45, and (2) the EC_{50} of AO85 was 58 nM. The IC_{50} of AOs in gene knockdown has been determined to be between 70 and 220 nM (Grunweller et al., 2003), indicating that AO85 works efficiently in our *in vitro* splicing system. At 160 nM AO85, exon skipping was induced in approximately 80% of transcripts. In comparison with this, at most 70% of exon skipping has been induced by 500 nM 2′-O-methyl phosphorothioate AOs in another cell-free splicing reaction (Spitali et al., 2009). The recent efforts to improve exon skipping efficiency by optimizing the AO sequence, backbone chemistry, and additional modifications (Kurreck et al., 2002) are worthwhile. Considering that AO85 has low EC_{50} (58.0 nM) (Fig. 3b), high exon skipping efficiency (80%) (Fig. 3b), and ability to induce exon 45 skipping in cultured human muscle cells (Takagi et al., 2004b), we believe that AO85 has high potential for clinical use. However, further studies are necessary before clinical use.

Acknowledgments

We would like to thank Ms. Kanako Yokoyama for her administrative assistance. This work was supported by a grant from the New Energy and Industrial Technology Development Organization, a Grant-in-Aid for Scientific Research (B) and a Grant-in-Aid for Exploratory Research from the Japan Society for the Promotion of Science, a Health and Labour Sciences Research Grant for Research on Psychiatric and Neurological Diseases and Mental Health, and a research grant for Nervous and Mental Disorders from the Ministry of Health, Labour, and Welfare, Japan.

Author Disclosure Statement

No competing financial interests exist.

References

AARTSMA-RUS, A. (2010). Antisense-mediated modulation of splicing: therapeutic implications for duchenne muscular dystrophy. RNA Biol. **7**, 453–461.

AARTSMA-RUS, A., FOKKEMA, I., VERSCHUUREN, J., GINJAAR, I., VAN DEUTEKOM, J., VAN OMMEN, G.J., and DEN DUNNEN, J.T. (2009a). Theoretic applicability of antisense-mediated exon skipping for Duchenne muscular dystrophy mutations. Hum. Mutat. **30**, 293–299.

AARTSMA-RUS, A., VAN VLIET, L., HIRSCHI, M., JANSON, A.A., HEEMSKERK, H., DE WINTER, C.L., DE KIMPE, S., VAN DEUTEKOM, J.C., T HOEN, P.A., and VAN OMMEN, G.J. (2009b). Guidelines for antisense oligonucleotide design and insight into splice-modulating mechanisms. Mol. Ther. **17**, 548–553.

BENNETT, C.F., and SWAYZE, E.E. (2010). RNA targeting therapeutics: molecular mechanisms of antisense oligonucleotides as a therapeutic platform. Ann. Rev. Pharmacol. Toxicol. **50**, 259–293.

DUAN, M., ZHOU, Z., LIN, R.X., YANG, J., XIA, X.Z., and WANG, S.Q. (2008). *In vitro* and *in vivo* protection against the

highly pathogenic H5N1 influenza virus by an antisense phosphorothioate oligonucleotide. Antivir. Ther. **13,** 109–114.

FLANIGAN, K.M., DUNN, D.M., VON NIEDERHAUSERN, A., SOLTANZADEH, P., HOWARD, M.T., SAMPSON, J.B., SWOBODA, K.J., BROMBERG, M.B., MENDELL, J.R., TAYLOR, L., et al. (2011). Nonsense mutation-associated Becker muscular dystrophy: interplay between exon definition and splicing regulatory elements within the DMD gene. Hum. Mutat. **32,** 299–308.

FREIER, S.M., and ALTMANN, K.H. (1997). The ups and downs of nucleic acid duplex stability: structure-stability studies on chemically-modified DNA:RNA duplexes. Nucleic Acids Res. **25,** 4429–4443.

GOEMANS, N.M., TULINIUS, M., VAN DEN AKKER, J.T., BURM, B.E., EKHART, P.F., HEUVELMANS, N., HOLLING, T., JANSON, A.A., PLATENBURG, G.J., SIPKENS, J.A., et al. (2011). Systemic administration of PRO051 in Duchenne's muscular dystrophy. N. Eng. J. Med. **364,** 1513–1522.

GRUNWELLER, A., WYSZKO, E., BIEBER, B., JAHNEL, R., and ERDMANN, V.A., KURRECK, J. (2003). Comparison of different antisense strategies in mammalian cells using locked nucleic acids, 2'-O-methyl RNA, phosphorothioates and small interfering RNA. Nucleic Acids Res. **31,** 3185–3193.

HABARA, Y., DOSHITA, M., HIROZAWA, S., YOKONO, Y., YAGI, M., TAKESHIMA, Y., and MATSUO, M. (2008). A strong exonic splicing enhancer in dystrophin exon 19 achieve proper splicing without an upstream polypyrimidine tract. J. Biochem. **143,** 303–310.

HABARA, Y., TAKESHIMA, Y., AWANO, H., OKIZUKA, Y., ZHANG, Z., SAIKI, K., YAGI, M., and MATSUO, M. (2009). *In vitro* splicing analysis showed that availability of a cryptic splice site is not a determinant for alternative splicing patterns caused by +1G—>A mutations in introns of the dystrophin gene. J. Med. Genet. **46,** 542–547.

HICKS, M.J., LAM, B.J., and HERTEL, K.J. (2005). Analyzing mechanisms of alternative pre-mRNA splicing using *in vitro* splicing assays. Methods **37,** 306–313.

KURRECK, J., WYSZKO, E., GILLEN, C., and ERDMANN, V.A. (2002). Design of antisense oligonucleotides stabilized by locked nucleic acids. Nucleic Acids Res. **30,** 1911–1918.

LU, Q.L., YOKOTA, T., TAKEDA, S., GARCIA, L., MUNTONI, F., and PARTRIDGE, T. (2011). The status of exon skipping as a therapeutic approach to duchenne muscular dystrophy. Mol. Ther. **19,** 9–15.

MATHEWS, D.H., SABINA, J., ZUKER, M., and TURNER, D.H. (1999). Expanded sequence dependence of thermodynamic parameters improves prediction of RNA secondary structure. J. Mol. Biol. **288,** 911–940.

MORITA, K., HASEGAWA, C., KANEKO, M., TSUTSUMI, S., SONE, J., ISHIKAWA, T., IMANISHI, T., and KOIZUMI, M. (2001). 2'-O,4'-C-ethylene-bridged nucleic acids (ENA) with nuclease-resistance and high affinity for RNA. Nucleic Acids Res. Suppl. **1,** 241–242.

NASIM, M.T., CHOWDHURY, H.M., and EPERON, I.C. (2002). A double reporter assay for detecting changes in the ratio of spliced and unspliced mRNA in mammalian cells. Nucleic Acids Res. **30,** e109.

PAN, W.H., and CLAWSON, G.A. (2006). Antisense applications for biological control. J. Cell Biochem. **98,** 14–35.

PANDYA-JONES, A., and BLACK, D.L. (2009). Co-transcriptional splicing of constitutive and alternative exons. RNA **15,** 1896–1908.

PARTRIDGE, T. (2010). The potential of exon skipping for treatment for Duchenne muscular dystrophy. J Child Neurol. **25,** 1165–1170.

PEREZ, B., RODRIGUEZ-PASCAU, L., VILAGELIU, L., GRINBERG, D., UGARTE, M., and DESVIAT, L.R. (2010). Present and future of antisense therapy for splicing modulation in inherited metabolic disease. J. Inherit. Metab. Dis. **33,** 397–403.

POPPLEWELL, L.J., TROLLET, C., DICKSON, G., and GRAHAM, I.R. (2009). Design of phosphorodiamidate morpholino oligomers (PMOs) for the induction of exon skipping of the human DMD gene. Mol. Ther. **17,** 554–561.

PRAMONO, Z.A., TAKESHIMA, Y., ALIMSARDJONO, H., ISHII, A., TAKEDA, S., and MATSUO, M. (1996). Induction of exon skipping of the dystrophin transcript in lymphoblastoid cells by transfecting an antisense oligodeoxynucleotide complementary to an exon recognition sequence. Biochem. Biophys. Res. Commun. **226,** 445–449.

SHIGA, N., TAKESHIMA, Y., SAKAMOTO, H., INOUE, K., YOKOTA, Y., YOKOYAMA, M., and MATSUO, M. (1997). Disruption of the splicing enhancer sequence within exon 27 of the dystrophin gene by a nonsense mutation induces partial skipping of the exon and is responsible for Becker muscular dystrophy. J. Clin. Invest. **100,** 2204–2210.

SPITALI, P., RIMESSI, P., FABRIS, M., PERRONE, D., FALZARANO, S., BOVOLENTA, M., TRABANELLI, C., MARI, L., BASSI, E., TUFFERY, S., et al. (2009). Exon skipping-mediated dystrophin reading frame restoration for small mutations. Hum. Mutat. **30,** 1527–1534.

STAHEL, R.A., and ZANGEMEISTER-WITTKE, U. (2003). Antisense oligonucleotides for cancer therapy-an overview. Lung Cancer **41 Suppl 1,** S81–S88.

SURONO, A., TRAN, V.K., TAKSHIMA, Y., WADA, H., YAGI, M., TAKAGI, M., KOIZUMI, M., and MATSUO, M. (2004). Chimeric RNA/ethylene bridged nucleic acids promote dystrophin expression in myocytes of Duchenne muscular dystrophy by inducing skipping of the nonsense-mutation-encoding exon. Hum. Gene Ther. **15,** 749–757.

TAKAGI, M., MORITA, K., NAKAI, D., NAKAGOMI, R., TOKUI, T., and KOIZUMI, M. (2004a). Enhancement of the inhibitory activity of oatp antisense oligonucleotides by incorporation of 2'-O,4'-C-ethylene-bridged nucleic acids (ENA) without a loss of subtype selectivity. Biochemistry **43,** 4501–4510.

TAKAGI, M., YAGI, M., ISHIBASHI, K., TAKESHIMA, Y., SURONO, A., MATSUO, M., and KOIZUMI, M. (2004b). Design of 2'-O-Me RNA/ENA chimera oligonucleotides to induce exon skipping in dystrophin pre-mRNA. Nucleic Acids Symp. Ser. (Oxf), **48,** 297–298.

TAKESHIMA, Y., YAGI, M., and MATSUO, M. (2011). Optimizing RNA/ENA chimeric antisense oligonucleotides using *in vitro* splicing. In: Exon Skipping: Methods and Protocols: Methods in Molecular Biology. A. Aartsma-Rus, ed. (Humana Press, New Jersey) in press.

TAKESHIMA, Y., NISHIO, H., SAKAMOTO, H., NAKAMURA, H., and MATSUO, M. (1995). Modulation of *in vitro* splicing of the upstream intron by modifying an intra-exon sequence which is deleted from the dystrophin gene in dystrophin Kobe. J. Clin. Invest. **95,** 515–520.

TAKESHIMA, Y., YAGI, M., OKIZUKA, Y., AWANO, H., ZHANG, Z., YAMAUCHI, Y., NISHIO, H., and MATSUO, M. (2010). Mutation spectrum of the dystrophin gene in 442 Duchenne/Becker muscular dystrophy cases from one Japanese referral center. J. Hum. Genet. **55,** 379–388.

TAKESHIMA, Y., YAGI, M., WADA, H., ISHIBASHI, K., NISHIYAMA, A., KAKUMOTO, M., SAKAEDA, T., SAURA, R., OKUMURA, K., and MATSUO, M. (2006). Intravenous infusion of an antisense oligonucleotide results in exon skip-

ping in muscle dystrophin mRNA of Duchenne muscular dystrophy. Pediatr. Res. **59,** 690–694.

TRAN, V.K., TAKESHIMA, Y., ZHANG, Z., YAGI, M., NISHIYAMA, A., HABARA, Y., and MATSUO, M. (2006). Splicing analysis disclosed a determinant single nucleotide for exon skipping caused by a novel intra-exonic four-nucleotide deletion in the dystrophin gene. J. Med. Genet. **43,** 924–930.

VAN AERSCHOT, A. (2006). Oligonucleotides as antivirals: dream or realistic perspective? Antivir. Res. **71,** 307–316.

VEEDU, R.N., and WENGEL, J. (2010). Locked nucleic acids: promising nucleic acid analogs for therapeutic applications. Chem. Biodivers **7,** 536–542.

WARD, A.J., and COOPER, T.A. (2010). The pathobiology of splicing. J. Pathol. **220,** 152–163.

WOOD, M.J., GAIT, M.J., and YIN, H. (2010). RNA-targeted splice-correction therapy for neuromuscular disease. Brain **133,** 957–972.

YAGI, M., TAKESHIMA, Y., SURUNO, A., TAKAGI, M., KOIZUMI, M., and MATSUO, M. (2004). Chimeric RNA and 2′-O, 4′-C-ethylene-bridged nucleic acids have stronger activity than phosphorothioate oligodeoxynucleotides in induction of exon-19 skipping in dystropin mRNA. Oligonucleotides **14,** 33–40.

ZHENG, Z.M., and BAKER, C.C. (2000). Parameters that affect *in vitro* splicing of bovine papillomavirus type 1 late pre-mRNAs. J. Virol Methods **85,** 203–214.

ZHU, J., KREN, B.T., PARK, C.W., BILGIM, R., WONG, P.Y., and STEER, C.J. (2007). Erythroid-specific expression of beta-globin by the sleeping beauty transposon for Sickle cell disease. Biochemistry **46,** 6844–6858.

ZUKER, M. (2003). Mfold web server for nucleic acid folding and hybridization prediction. Nucleic Acids Res. **31,** 3406–3415.

Address correspondence to:
Prof. Masafumi Matsuo
Department of Medical Rehabilitation
Faculty of Rehabilitation
Kobegakuin University
518 Arise, Ikawadani
Nishi
Kobe 651-2180
Japan

E-mail: mmatsuo@reha.kobegakuin.ac.jp

Received for publication June 17, 2011; accepted after revision August 22, 2011.

nature COMMUNICATIONS

OPEN

ARTICLE

Received 14 Jan 2011 | Accepted 11 Apr 2011 | Published 10 May 2011

DOI: 10.1038/ncomms1306

Chemical treatment enhances skipping of a mutated exon in the *dystrophin* gene

Atsushi Nishida[1,*], Naoyuki Kataoka[2,*], Yasuhiro Takeshima[1], Mariko Yagi[1], Hiroyuki Awano[1], Mitsunori Ota[1], Kyoko Itoh[3], Masatoshi Hagiwara[4,5] & Masafumi Matsuo[1]

Duchenne muscular dystrophy (DMD) is a fatal muscle wasting disease caused by a loss of the dystrophin protein. Control of dystrophin mRNA splicing to convert severe DMD to a milder phenotype is attracting much attention. Here we report a dystrophinopathy patient who has a point mutation in exon 31 of the *dystrophin* gene. Although the mutation generates a stop codon, a small amount of internally deleted, but functional, dystrophin protein is produced in the patient cells. An analysis of the mRNA reveals that the mutation promotes exon skipping and restores the open reading frame of dystrophin. Presumably, the mutation disrupts an exonic splicing enhancer and creates an exonic splicing silencer. Therefore, we searched for small chemicals that enhance exon skipping, and found that TG003 promotes the skipping of exon 31 in the endogenous *dystrophin* gene in a dose-dependent manner and increases the production of the dystrophin protein in the patient's cells.

[1] Department of Pediatrics, Kobe University Graduate School of Medicine, Chuo, 7-5-1 Kusunoki-cho, Kobe 650-0017, Japan. [2] Medical Top Track Program, Medical Research Institute, Tokyo Dental and Medical University, Tokyo 113-8510, Japan. [3] Department of Pathology and Applied Neurobiology, Graduate School of Medical Science, Kyoto Prefectural University of Medicine, Kyoto 602-8566, Japan. [4] Department of Functional Genomics, Tokyo Dental and Medical University, Tokyo 113-8510, Japan. [5] Department of Anatomy and Developmental Biology, Graduate School of Medicine, Kyoto University, Yoshida-Konoe-cho, Sakyo-ku, Kyoto 606-8501, Japan. *These authors contributed equally to this work. Correspondence and requests for materials should be addressed to M.H. (email: hagiwara.masatoshi.8c@kyoto-u.ac.jp) or to M.M. (email: matsuo@kobe-u.ac.jp).

Duchenne muscular dystrophy (DMD) is the most common inherited muscle disease and is caused by a mutation in the *dystrophin* gene, the largest in the human genome, on the X chromosome[1]. Because of progressive muscle wasting, DMD patients usually succumb to cardiac or respiratory failure in their twenties. Becker muscular dystrophy (BMD) is a milder allelic variant of DMD, usually affecting adult males. A reading frame rule explains the difference between DMD and BMD. Nonsense mutations or deletions causing frame shifts in the dystrophin mRNA, both of which create premature termination codons (PTCs), usually result in a severe DMD phenotype, because of a lack of the dystrophin protein. In contrast, mutations/deletions that maintain the original reading frame in the mRNA cause the milder BMD phenotype, as a mutated, but still functional, dystrophin protein can be expressed from the mRNA[2]. However, in some mild BMD cases, the patients had nonsense mutations in exons but still produced novel in-frame dystrophin mRNAs by skipping the exons containing the nonsense codon[3–7]. Thus, internally deleted but partially functional dystrophin proteins can be produced from the exon-skipped mRNAs.

The current major therapeutic approach established by us, as well as by other groups, is to convert DMD to BMD phenotypes by restoring dystrophin protein expression by inducing exon skipping with antisense oligonucleotides (AONs)[8–11]. Several different AONs have been designed against either splice sites or splicing enhancer elements to induce exon skipping in cells of DMD patients. The AONs, which are designed to target those splicing elements, were demonstrated to restore the reading frame of dystrophin by causing skipping of the target exons. For example, the administration of an AON against an exonic splicing enhancer (ESE) in exon 19 promoted exon skipping in cells and increased production of an internally deleted dystrophin protein[12–14]. Another AON against exon 51 is currently under clinical trials[9,15,16]. However, considering the therapeutic cost and convenience, small chemical compounds have been highly awaited. A small compound PTC124 (refs 17 and 18), which induces read-through of the PTC, was reported to have the potential to treat some DMD patients who have nonsense mutations. Although a clinical trial of PTC124 for DMD patients who have nonsense mutations in the *dystrophin* gene was completed, no significant improvement of treated patients was observed (http://www.ptcbio.com/May_DBMD_Trial_Update.htm).

We have been interested in the role of phosphorylation of SR proteins in splicing regulation. SR proteins are heavily phosphorylated in cells and are involved in constitutive and alternative splicing[19,20]. By extensive screening of 100,000 chemical compounds in a chemical library using *in vitro* phosphorylation assay, we identified several synthetic chemical compounds that inhibit SR protein kinases specifically. We first identified a synthetic compound as a specific inhibitor of SR protein kinases and named it as SRPIN340 (ref. 21). Administration of SRPIN340 to mice retina changed the splicing pattern of vascular endothelial growth factor-A and suppressed vascular generation[22]. We next identified TG003, a kinase inhibitor specific for Cdc-like kinases (Clks)[22] that are also able to phosphorylate SR proteins. TG003 affected splicing both *in vitro* and *in vivo*[23,24]. Recently, we reported that spliceostatin, originally characterized as an antitumour drug, blocked splicing and promoted the export of unspliced pre-mRNAs[25,26].

Here we tested these compounds to determine whether splicing in this context in *ex vivo* myoblast cell culture could be modified, and found that TG003 enhanced exon skipping and produced an internally deleted dystrophin protein in the *in vitro*-formed myotubes of a dystrophinopathy patient who has a point mutation in exon 31 of the *dystrophin* gene.

Results

Point mutation causes skipping of exon 31 in a DMD patient. We have analysed and identified mutations in the *dystrophin* gene of more than 400 dystrophinopathy patients. We found that one patient (KUCG797) had a point mutation in exon 31. The mutation is a change from G to T (G to U on RNA) at position 4303 of the dystrophin cDNA (c.4303G>T, Fig. 1a). As this change replaced GAG for glutamate with the TAG for a stop codon (p.Glu1435X), the patient was not expected to produce dystrophin, resulting in severe DMD. The immunostaining of a biopsied skeletal muscle, however, showed patchy and discontinuous signals with antibodies recognizing N- or C-terminal dystrophin domains (Fig. 1e,f), which are comparable to BMD. Size and shape of muscle fibres were heterogeneous.

To explain the discrepancy between the genotype and the immunostaining pattern, we presumed that the nonsense mutation in exon 31 disrupted the ESE, which resulted in skipping of the mutated exon in the patient's muscle cells. To test this possibility, we analysed the *dystrophin* mRNA in skeletal muscle. The reverse transcription polymerase chain reaction (RT–PCR) amplification of the region extending from exon 27 to exon 32 showed two nearly equal amounts of two products: one of expected size with exons 27–32, including the TAG stop codon in exon 31, and the other a smaller product lacking exon 31 (Fig. 1h,i). However, the other introns of this *dystrophin* gene, which consists of 79 exons, seemed to be correctly spliced out (Supplementary Fig. S1, (−) lanes and Supplementary Table S1). The resulting dystrophin mRNA lacking the 111-bp-long exon 31 was in-frame to produce an internally deleted, but likely functional, dystrophin protein.

In the patient's muscle cells, the exon 31-containing mRNA should be lost by NMD, and only the internally deleted protein transcribed from the exon 31-skipped transcript can be expressed. Therefore, the dystrophin protein was immunostained with antibodies against the N- or C-terminal domains of dystrophin (Fig. 1b,c,e,f), but failed to be recognized by MANDYS1, a monoclonal antibody against the exon 31-encompassing region in the patient's cells (Fig. 1d,g).

Splicing regulators involved in exon 31 splicing. These results suggest that the point mutation in exon 31 not only produces a stop codon but also modifies an exonic splicing regulatory site. To test this hypothesis, we incorporated the wild-type and mutant *dystrophin* gene fragment that retains exon 31 and the flanking introns into the H492 vector, which has been used for splicing analysis in cells (Fig. 1j)[27–29], and transfected them into HeLa cells. Two PCR products were detected with the mutant plasmid (Fig. 1k), whereas only a single RT–PCR product was amplified from the wild-type plasmid. Sequencing analysis revealed that the smaller PCR product from the mutant does not include exon 31 (data not shown).

As mutant exon 31 with flanking introns cloned into the H492 vector is sufficient to promote skipping, we tried to identify the splicing regulatory factors that bind to the RNA portion. According to the SpliceAid program (http://www.introni.it/splicing.html)[30], exon 31 has the binding sequence of SRp30c/SRSF9 identified by SELEX (Supplementary Fig. S2b)[31]. The point mutation found in the patient disrupts the binding site of SRp30c/SRSF9, a member of the SR protein family (Supplementary Fig. S2a), which are often purine-rich and known to bind to ESEs. In addition, the mutation presumably generates an RNA sequence that has high homology to exonic splicing silencers (ESSs) recognized by the heterogeneous nuclear ribonucleoproteins (hnRNPs) A1 (Supplementary Fig. S2a,b)[32]. To test this notion, we first compared the binding to hnRNP A1 of the mutant RNA with that of the wild-type RNA in a gel mobility shift assay. The recombinant hnRNP A1 was prepared as a glutathione *S*-transferase (GST)-tagged protein (Supplementary Fig. S3b, lane 3) and mixed with either the wild-type or mutant dystrophin RNA, and the resultant complexes were analysed by native polyacrylamide gel electrophoresis. As shown in Figure 2a, two hnRNP A1–RNA complexes showed different patterns of migration on the gel